Dynamical two-point correlation functions in a high-temperature Heisenberg paramagnet*†

Charles W. Myles‡
Arthur Holly Compton Laboratory of Physics, Washington University, St. Louis, Missouri 63130 and Battelle Memorial Institute, § 505 King Avenue, Columbus, Ohio 43201

Peter A. Fedders
Arthur Holly Compton Laboratory of Physics, Washington University, St. Louis, Missouri 63130
(Received 18 December 1973)

The dynamical two-point correlation functions of the high-temperature Heisenberg paramagnet as described by nonlinear integral equations generated by moment expansions developed by Reiter are investigated. In particular, equations for the magnetic dipole correlation functions and magnetic quadrupole correlation functions are obtained and solved in a lowest-order self-consistent approximation. These correlation functions are directly measurable in electromagnetic, neutron-scattering, and acoustic experiments in dense magnetic insulators. From the solution for the dipole correlation functions, theoretical values for the spin-diffusion coefficient and the exchange-narrowed dipolar linewidth are obtained which are within 12% and 22%, respectively, of the measured values for $RbMnF_3$.

I. INTRODUCTION

While the static or thermodynamic properties of high-temperature paramagnetic insulators are well understood, much less is known about their dynamical properties. Until recently, most theoretical work on such systems was limited to the fitting of an assumed line-shape function to its first few moments.[1,2] This type of analysis has been employed extensively in calculating NMR and EPR linewidths and spin-diffusion coefficients.[3–5] Recently, diagrammatic expansions have been developed for calculating, in principle, all of the moments of the line-shape function for the Heisenberg paramagnet.[4,5] In practice, however, it is impossible to calculate more than the first few moments by these methods because of the increasing number and complexity of the diagrams for the higher moments. Although the method of fitting moments has been very popular and usually gives reasonable qualitative results, it is highly arbitrary and can always be made to give correctly a single experimental linewidth, as is discussed in Sec. II B of Ref. 6. In addition, recent NMR, EPR, and APR (acoustic paramagnetic resonance) measurements show that qualitative,[3,7] and sometimes quantitative,[8] fits to line shapes cannot be obtained from simple functions, even at high temperatures. Starting with Bennett and Martin,[9] progress has recently been made in obtaining equations for line-shape functions which are derived from microscopic equations of motion.[4–6,9–13] Although different starting points have been used by different workers, the final equations obtained are in many cases identical or almost identical to each other.

It is the purpose of this paper to investigate a self-consistent perturbation scheme for the experimentally measurable two-point time-dependent correlation functions of the high-temperature Heisenberg paramagnet and to obtain and solve the lowest-order equations self-consistently. An equation for the dipole-dipole spin correlation function for the isotropic-exchange high-temperature Heisenberg paramagnet, which is measureable in EPR, NMR, and neutron-scattering experiments in dense magnetic insulators,[7,14,15] has already been obtained[11] in this lowest-order approximation. The new results presented in this paper are the inclusion of the dipolar interaction in order to calculate the exchange narrowed EPR linewidth for the dipole-dipole spin correlation function and the calculation of one of the quadrupole-quadrupole spin correlation functions, which is observable in acoustic experiments.[16] In addition, we shall exhibit a particularly simple method of solving the integral equations for both correlation functions which reproduces all moments and the long-wavelength diffusive behavior to lowest order in $1/c$, where c is the interaction range of the Heisenberg interaction. Since the original lowest-order equation is not even exact to order $1/c$, very little useful information is lost by using this additional approximation.

The rest of this section will be devoted to a discussion of the types of correlation functions to be considered and to a discussion of our notation. In Sec. II we discuss the general method of calculation for the isotropic high-temperature Heisenberg paramagnet and obtain explicit integral equations for the relevant correlation functions in a lowest-order approximation. The equations are also generalized to include effects due to an external field and the dipolar interaction. Section III contains explicit solutions for the correlation functions which are measureable in electromagnetic and acoustic experiments. A discussion of these

results along with predictions for the spin-diffusion coefficient and the exchange-narrowed dipolar linewidth contained in the dipole correlation function are presented and compared with experiments on $RbMnF_3$.

It is convenient to use irreducible tensor operators for a spin of magnitude S at a given site as discussed by Reiter.[5] The dipole and quadrupole operators are

$$A_{1,\pm1} = \mp [2S(S+1)/3]^{-1/2} S_\pm , \tag{1a}$$

$$A_{1,0} = [S(S+1)/3]^{-1/2} S_z , \tag{1b}$$

$$A_{2,\pm2} = [2S(S+1)(2S-1)(2S+3)/15]^{-1/2} S_\pm^2 , \tag{1c}$$

$$A_{2,\pm1} = \mp [2S(S+1)(2S-1)(2S+3)/15]^{-1/2} \{S_\pm, S_z\} , \tag{1d}$$

$$A_{2,0} = [S(S+1)(2S-1)(2S+3)/45]^{-1/2} \times [S_z^2 - \tfrac{1}{3}S(S+1)] , \tag{1e}$$

where S_i is the ith component of the spin dipole operator, $S_\pm = S_x \pm iS_y$, and the curly brackets in Eq. (1d) denote the anticommutator. All of the operators are normalized to $\mathrm{Tr}\,|A|^2 = (2S+1)$. In what follows we shall refer to $A_{lm} = A_\alpha$, where $\alpha = (l, m)$.

In the high-temperature limit it is further convenient to define a set of two-point time-dependent correlation functions as[17]

$$G_{\alpha\beta}(\vec{l}, \vec{l}'; t, t') = \langle A_\alpha(\vec{l}, t) A_\beta^\dagger(\vec{l}', t') \rangle \Theta(t - t'), \tag{2}$$

where $\vec{l}$ denotes a lattice site, the angular brackets $\langle X \rangle$ denote the average value of X in the canonical ensemble, and $\Theta(t)$ is the step function. Since the system is translationally invariant in time and has the invariance of a crystal lattice under translations through a lattice vector, G can be transformed according to the usual prescription[6]

$$G(\vec{l} - \vec{l}', t - t') = \frac{1}{N} \sum_{\vec{q}} \int_{-\infty}^{\infty} \frac{d\omega}{2\pi} G(\vec{q}, \omega) \times e^{i\vec{q}\cdot(\vec{l} - \vec{l}') - i\omega(t - t')} , \tag{3}$$

where N is the number of lattice sites and the summation is over all wave vectors $\vec{q}$ in the first Brillouin zone.

$G_{\alpha\beta}(\vec{q}, \omega)$ can be related to other frequency-dependent correlation functions[18] by means of the fluctuation-dissipation theorem. The components of the usual dynamic susceptibility[3,11] or dipole-dipole response function are proportional to $G_{\alpha\beta}(\vec{q}, \omega)$ with $\alpha = \beta = (1, m)$. Acoustic attenuation due to single-ion magnetostriction[19] is proportional to $G_{\alpha\beta}(\vec{q}, \omega)$, with $\alpha = (2, m)$ and $\beta = (2, m')$. Single ion magnetostriction corresponds to a modulation of a local anisotropy energy and can be described by terms in a Hamiltonian proportional to

$$A_{2,m}(\vec{l}, t) Q ,$$

where Q is a phonon normal coordinate. Volume magnetostriction[19] corresponds to the modulation of a spin-spin interaction and can be described by terms in a Hamiltonian proportional to

$$A_{1,m}(\vec{l}_1, t) A_{1,m'}(\vec{l}_2, t) Q ,$$

where $\vec{l}_1 \neq \vec{l}_2$. The appropriate correlation function describing the acoustic attenuation due to this process is[16]

$$\langle A_{1,m_1}(\vec{l}, t) A_{1,m_2}(\vec{l}_2, t) A_{1,m_3}(\vec{l}_3, t') A_{1,m_4}(\vec{l}_4, t') \rangle \Theta(t - t') .$$

This form of correlation function is not of the type that will be considered in this paper, but will be dealt with in a later publication.

II. METHOD

It is often convenient to express $G_{\alpha\beta}(\vec{q}, \omega)$ in terms of a mass operator or self-energy $\Sigma_{\alpha\beta}(\vec{q}, \omega)$. For the correlation function defined by Eq. (2), in the high-temperature limit, such an operator is defined by the equation

$$i \frac{\partial}{\partial t} G_{\alpha\beta}(\vec{q}, t) - \int dt' \Sigma_{\alpha\gamma}(\vec{q}, \bar{t} - \bar{t}) G_{\gamma\beta}(\vec{q}, \bar{t}) = i\delta_{\alpha\beta}\delta(t) \tag{4a}$$

or

$$\omega G_{\alpha\beta}(\vec{q}, \omega) - \Sigma_{\alpha\gamma}(\vec{q}, \omega) G_{\gamma\beta}(\vec{q}, \omega) = i\delta_{\alpha\beta} , \tag{4b}$$

where repeated Greek subscripts are summed over, and $\Sigma(t)$ is proportional to $\Theta(t)$. Of course one can always define Σ through Eqs. (4). However, whether or not this is a useful procedure depends on the particular problem. Often one tries to obtain an expansion of Σ in terms of G. This leads to a self-consistent Wigner-Brillouin-type perturbation theory as is common with interacting fermion or boson problems.[17] It is not clear, however, whether such an expansion exists for the Heisenberg paramagnet. The conditions under which such an expansion is valid for the Heisenberg system are discussed below. Another advantage of the representation of G in terms of Σ is that a small amount of structure in Σ can lead to a large amount of structure in G.[6]

The frequency moments of G and Σ are defined as

$$M_{\alpha\beta}(\vec{q}, n) = \int_{-\infty}^{\infty} \frac{d\omega}{\pi} \omega^n G_{\alpha\beta}(\vec{q}, \omega) , \tag{5a}$$

$$L_{\alpha\beta}(\vec{q}, n) = \int_{-\infty}^{\infty} \frac{d\omega}{\pi} \omega^{n-2} \Sigma_{\alpha\beta}(\vec{q}, \omega) . \tag{5b}$$

A particularly useful expansion for G and Σ in terms of these moments is

$$G_{\alpha\beta}(\vec{q}, t) = \sum_{n=0}^{\infty} \frac{(-it)^n}{n!} M_{\alpha\beta}(\vec{q}, n) \Theta(t) , \tag{5c}$$

$$\Sigma_{\alpha\beta}(\vec{q}, t) = -i \sum_{n=0}^{\infty} \frac{(-it)^n}{n!} L_{\alpha\beta}(\vec{q}, n+2) \Theta(t)$$

$$+L_{\alpha\beta}(\vec{q}, 1)\,\delta(t)\ . \tag{5d}$$

These equations may also be written in frequency space as

$$G_{\alpha\beta}(\vec{q}, z) = i\sum_{n=0}^{\infty} M_{\alpha\beta}(\vec{q}, n)/z^{n+1}\ , \tag{6a}$$

$$\Sigma_{\alpha\beta}(\vec{q}, z) = \sum_{n=0}^{\infty} L_{\alpha\beta}(\vec{q}, n+2)/z^{n+1} + L_{\alpha\beta}(\vec{q}, 1), \tag{6b}$$

where z is, in general, complex. By substituting Eqs. (5) into Eq. (4a) and matching powers of t, one obtains

$$M_{\alpha\beta}(\vec{q}, n+1) = \sum_{m=1}^{n+1} L_{\alpha\gamma}(\vec{q}, m) M_{\gamma\beta}(\vec{q}, n+1-m)\ . \tag{7}$$

This equation has the following diagrammatic interpretation[5]: If $L_{\alpha\beta}(\vec{q}, n)$ corresponds to an irreducible[20] set of diagrams of order n with one $\vec{q}$ line in and one $\vec{q}$ line out, then $M_{\alpha\beta}(\vec{q}, n)$ corresponds to all connected diagrams (reducible and irreducible) of order n that are made up by connecting all $L_{\alpha\beta}(\vec{q}, k)$ with $k \leq n$, and have one $\vec{q}$ line in and one $\vec{q}$ line out. This is equivalent both to a multinomial expansion[21] of $M_{\alpha\beta}(\vec{q}, n)$ in terms of $L_{\alpha\beta}(\vec{q}, n)$ and (in the dipole-correlation-function case) to Reiter's diagrammatic expansion of $M_{\alpha\beta}(\vec{q}, n)$ in terms of $L_{\alpha\beta}(\vec{q}, n)$.

By extending the work of Resibois and De Leneer[4] and of Reiter,[5] one can formulate criteria for the existence of a self-energy which can be written as a functional of G. A skeleton diagram is defined as a diagram which cannot be made up by piecing together lower-order diagrams.[4,5] It is shown elsewhere[21] that such a functional for the self-ener-

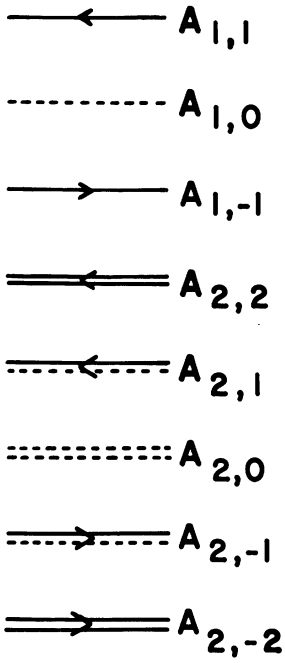

FIG. 1. The diagrammatic representation of the tensor spin operators at a given lattice site and a given time.

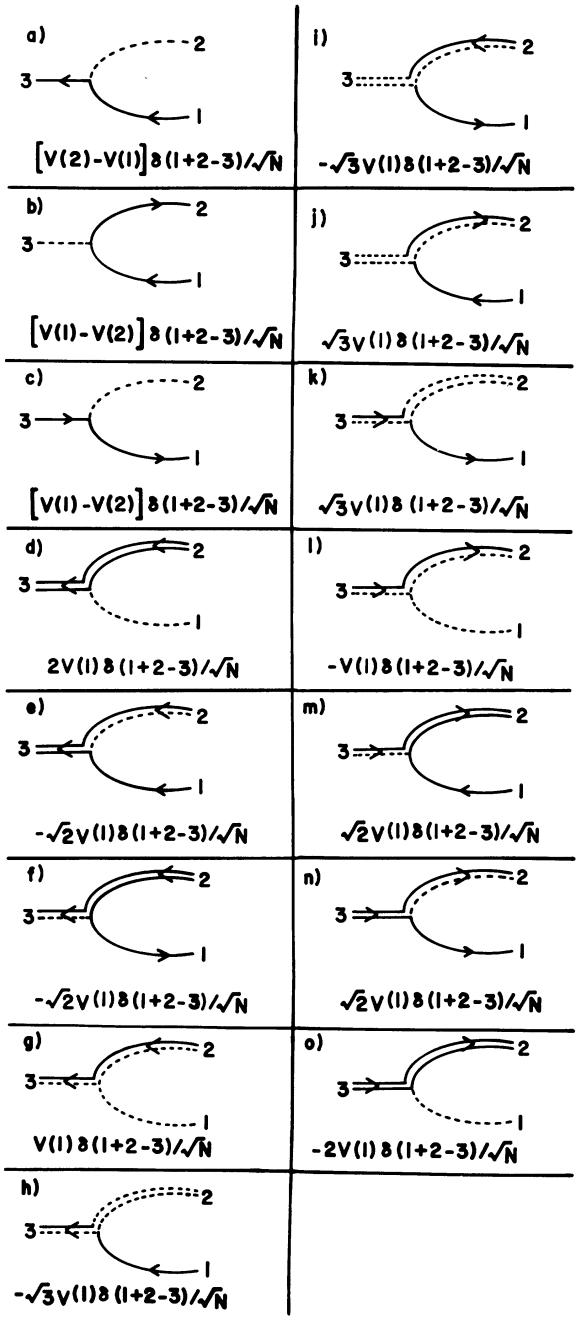

FIG. 2. The basic vertices for the spin-spin interaction and their corresponding analytic expressions. The operators are at wave vectors $\vec{q}$ and the vertex is at time t. $V(\vec{1}, \vec{1}')$ as defined in Eq. (9) acts at the vertex and the abbreviations $\vec{q}_1 = 1$, $\vec{q}_2 = 2$, $\vec{q}_3 = 3$ have been used.

gy $\Sigma(t)$ can be obtained by replacing all of the lines in all skeleton diagrams for L with G's and by integrating timewise over the internal vertices. This will be a valid procedure if and only if every diagram for M or L is multiplied by the number of ways its vertices can be time ordered. Therefore, as is discussed below, the diagrams for Σ are the infinite-temperature skeleton diagrams of Reiter[5] for the moments L with the internal lines replaced by G's. Effectively, then, the diagrams that we will use in our calculation of Σ and G are the resummation of a selected infinite subset of Reiter's[5] diagrams. Such a resummation or renormalization of the basic diagrams was first suggested by Reiter[5] for the dipole correlation function.

Initially, we consider the high-temperature Heisenberg paramagnet with only isotropic exchange and no external magnetic field. The Hamiltonian for this system is

$$H = -\tfrac{1}{2}\Sigma_{\vec{l},\vec{l}'} J(\vec{l}-\vec{l}')\,\vec{S}(\vec{l},t)\cdot\vec{S}(\vec{l}',t)\ , \tag{8}$$

where $\vec{S}(\vec{l},t)$ is the spin operator at the lattice site $\vec{l}$ which evolves in time according to the Heisenberg representation, and $J(\vec{l}-\vec{l}')$ is the interaction energy between the spins at different sites $\vec{l}$ and $\vec{l}'$. We shall obtain integral equations for the correlation functions by first considering the diagrams for the moments and then by carrying out the procedure discussed above. The method used here for the moment diagrams is the same as that used by Reiter[5] except that it is generalized to include the quadrupole operators $A_{2,m}(\vec{l})$ as well as the dipole operators $A_{1,m}(\vec{l})$. The graphical representation of these operators is given in Fig. 1.

From matrix elements of the Liouville operator we form the basic vertices at infinite temperature exactly as Reiter[5] does. We will limit our discussion to only these basic vertices, since they give all of the moments exactly to order $1/c$, where c is the number of spins with which a given spin interacts.[21] The only vertices that contribute for the case of isotropic exchange are given along with their corresponding analytical expressions in Fig. 2. In that figure we have also used a reduced exchange energy defined by

$$V(\vec{l}_1-\vec{l}_2) = [S(S+1)/3]^{1/2} J(\vec{l}_1-\vec{l}_2)/\hbar \tag{9}$$

for the Fourier-transformed vertices.

The diagrams for the moments to order $1/c$ are constructed by putting together the basic vertices. The rules for generating the moments $L_{\alpha\beta}(\vec{q},n)$ and $M_{\alpha\beta}(\vec{q},n)$ are obtained from a generalization of the rules given by Reiter.[5] For $L_{\alpha\beta}(\vec{q},n)$ the rules are: (i) Draw all distinct irreducible diagrams with n vertices which can be made from the basic vertices which start with an α-type line and end with a β-type line. (ii) Label the initial and final lines by $\vec{q}$. Label all internal lines by $\vec{q}_i$. (iii) Associate the appropriate analytic expression from Fig. 2 with each vertex. (iv) Sum over all indices $\vec{q}_i$. The number of times a graph is counted is equal to the number of ways its internal vertices can be time ordered.

For the isotropic high-temperature paramagnet, only the diagonal correlation functions $G_{\alpha\alpha}(\vec{q},t)$ and diagonal self-energies $\Sigma_{\alpha\alpha}(\vec{q},t)$ are nonzero. From the preceding discussion and from Reiter's paper,[5] one can deduce that $\Sigma_{\alpha\alpha}(\vec{q},t)$ is given by the sum of all skeleton diagrams.[21] In each skeleton diagram the internal lines and vertices are labeled in the same way as for the moment diagrams, but in addition each vertex is labeled by a time t_i, with t being the first vertex and zero being the last. Each line labeled $\vec{q}_i$ and going from vertex t_k to t_j is replaced by $G_{\alpha\alpha}(\vec{q}_i, t_k - t_j)$, where α is the appropriate index from Fig. 1. All internal $\vec{q}_i$ are summed over, all internal times t_i are integrated over, and a given diagram is multiplied by $(-1)^{n_v+1}$, where n_v is the number of internal vertices. This scheme for obtaining the diagrams for Σ from those for its moments L amounts to an effective summation of a selected infinite subset of diagrams and is very similar to the renormalization schemes suggested by Reiter.[5]

Approximate equations for the correlation functions can be obtained by noting which skeleton diagrams are used. For the rest of this paper we shall only be concerned with the lowest-order approximation which consists of the lowest-order skeleton diagrams. These diagrams are the bubble diagrams formed from two vertices of the types given in Fig. 2. Typical bubble diagrams are shown in Fig. 3. For isotropic exchange with no

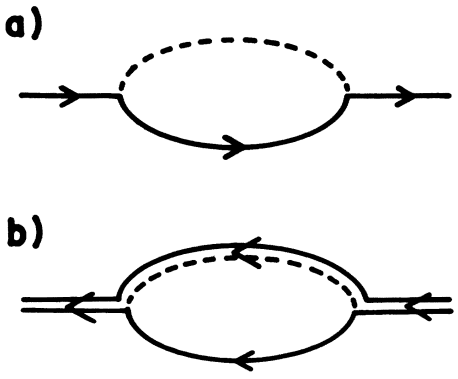

FIG. 3. Typical bubble diagrams for the calculation of the high-temperature moments of the two-point self-energy functions. (a) A typical bubble for a dipole-dipole self-energy moment. (b) A typical bubble for a quadrupole-quadrupole self-energy moment.

external magnetic field, all of the dipole correlation functions, $\alpha = (1, m)$, are equal and all of the quadrupole correlation functions, $\alpha = (2, m)$, are equal. Thus we shall denote these functions by G_1 and G_2, respectively, and denote their self-energies by Σ_1 and Σ_2. Using the previously discussed rules we obtain the lowest-order self-energies:

$$\Sigma_1(\vec{q}, t) = iN^{-1}\sum_{\vec{q}'}[V(\vec{q}') - V(\vec{q} - \vec{q}')]^2 \times G_1(\vec{q}', t)\, G_1(\vec{q} - \vec{q}', t), \tag{10}$$

$$\Sigma_2(\vec{q}, t) = 6iN^{-1}\sum_{\vec{q}'}[V(\vec{q}')]^2 G_1(\vec{q}, t)\, G_2(\vec{q} - \vec{q}', t). \tag{11}$$

These equations, along with Eq. (4a), form nonlinear integral equations for G_1 and G_2. Equation (10) is not new. It was first derived by Martin and Bennet[9] in an altered form and has been extensively studied by Blume and Hubbard[11] as well as other authors.[6] However, the use of these methods for quadrupolar correlation functions and Eq. (11) are new.

The inclusion of an external magnetic field in the Hamiltonian,

$$H' = -\mu H_0 S_z = -\hbar\omega_0 S_z\,, \tag{12}$$

causes only a minor change in the equations. Only one additional type of skeleton diagram is added, and that is a line corresponding to $A_{l,m}$ with a point on it which contributes $m\omega_0$ to the moments and which contributes $m\omega_0\delta(t)$ to the self-energy. Thus

$$\Sigma_{l,m}(\vec{q}, t) \to m\omega_0\delta(t) + \Sigma_{l,m}(\vec{q}, t) \tag{13}$$

with the addition of an external magnetic field.

Finally we wish to include the anisotropic dipolar interaction in order to calculate the exchange-narrowed EPR linewidth. This interaction is expressed as an additional term in the Hamiltonian of the form

$$H'' = -\tfrac{1}{2}\Sigma_{\vec{l}\vec{l}'} S_i(\vec{l}) I_{ij}(\vec{l} - \vec{l}')\, S_j(\vec{l}')\,, \tag{14}$$

$$I_{ij}(\vec{l}) = (\gamma_e\hbar)^2[\delta_{ij} - 3(l_i l_j/l^2)]/l^3\,, \tag{15}$$

where repeated Cartesian indices are summed over. The contribution of this dipolar interaction to the self-energy of the dipole and quadrupole correlation functions derived from diagrammatic rules is contained elsewhere.[21] The rules are a straightforward generalization of the rules for the isotropic case with many more basic vertices. The lowest-order (bubble) results for the dipole correlation function are the same as derived by one of us earlier[6] by another method. We assume that the isotropic exchange is much greater than the dipolar interaction energy and thus nondiagonal correlation functions can thus be neglected. From Ref. 6 the $\alpha = 1$ self-energy after Fourier transforming into frequency space is, in the present notation,

$$\begin{aligned}\Sigma_{1,1}(\vec{q}, \omega) = \frac{\gamma}{N}\sum_{\vec{q}'}\int_{-\infty}^{\infty}\frac{d\omega'}{2\pi}\Big(&[\tfrac{1}{2}J_{xx}(\vec{q}') + \tfrac{1}{2}J_{yy}(\vec{q}') - J_{zz}(\vec{q} - \vec{q}')]G_{1,1}(\vec{q}', \omega')G_{1,0}(\vec{q}' - \vec{q}, \omega - \omega') \\ &+ \tfrac{1}{2}\{J_{xz}(\vec{q}')[J_{xz}(\vec{q}') + J_{xz}(\vec{q}' - \vec{q})] + J_{yz}(\vec{q}')[J_{yz}(\vec{q}') + J_{yz}(\vec{q}' - \vec{q})]\}[G_{10}(\vec{q}', \omega')G_{10}(\vec{q}' - \vec{q}, \omega - \omega') \\ &+ G_{11}(\vec{q}', \omega')G_{11}(\vec{q}' - \vec{q}, \omega - \omega')] + \tfrac{1}{2}[J_{xz}^2(\vec{q}') + J_{yz}^2(\vec{q}')]G_{11}(\vec{q}, \omega')G_{11}(\vec{q}' - \vec{q}, \omega + \omega') \\ &+ \tfrac{1}{4}\{[J_{xx}(\vec{q}') - J_{yy}(\vec{q}')]^2 + 4J_{xz}^2(\vec{q}')\}G_{11}(\vec{q}', \omega')G_{10}(\vec{q}' - \vec{q}, \omega + \omega')\Big)\,,\end{aligned} \tag{16}$$

where

$$\gamma = [S(S+1)/3]^{1/2}/\hbar\,, \tag{17}$$

$$J_{ij}(\vec{l}) = J(\vec{l})\,\delta_{ij} + I_{ij}(\vec{l})\,. \tag{18}$$

The convergence of the diagrammatic perturbation theory and the validity of the lowest-order (bubble) result are not well understood at the present time and this point will be discussed in Sec. III. In addition, as was discussed previously, the lowest-order results can be derived in a number of ways. The derivation of the integral equations by Reiter's[5] method can easily be generalized to take into account higher-order terms in the self-energy at high temperatures. On the other hand, it is not clear how to generalize the method to temperatures near the transition temperature. Other methods[6,9,13] can be applied at all temperatures, although their validity is uncertain and it is unclear how to generalize them to include more terms in the self-energy.

III. RESULTS

A. Solution of equations

In this section we shall solve the nonlinear integral equations derived in Sec. II, and in Sec. III B we shall use the solution for the dipole correlation function to obtain the spin-diffusion coefficient and the exchange-narrowed dipolar linewidth. First, consider G_1 and G_2 for the high-temperature isotropic Heisenberg paramagnet. It is convenient to express both the G's and the Σ's in terms of spectral representations as

$$G_\alpha(\vec{q}, \omega) = i\int_{-\infty}^{\infty}\frac{d\omega'}{\pi}\frac{g_\alpha(\vec{q}, \omega')}{\omega - \omega' + i\epsilon}\,, \tag{19}$$

$$\Sigma_\alpha(\vec{q},\omega)=\int_{-\infty}^{\infty}\frac{d\omega'}{\pi}\frac{\Gamma_\alpha(\vec{q},\omega')}{\omega-\omega'+i\epsilon}+\Pi_\alpha(\vec{q},\omega)-i\Gamma_\alpha(\vec{q},\omega)\,, \tag{20}$$

where ϵ is an arbitrarily small positive quantity and α is 1 or 2. The quantity $g_\alpha(\vec{q},\omega)$ is the experimentally measured spectral function and is related to $\Sigma(\vec{q},\omega)$ through the equation

$$g_\alpha(\vec{q},\omega)=\Gamma_\alpha(\vec{q},\omega)/[(\omega-\Pi_\alpha(\vec{q},\omega))^2+(\Gamma_\alpha(\vec{q},\omega))^2]\,. \tag{21}$$

By Fourier transforming, it can be seen that Eqs. (10) and (11) are equivalent to the equations

$$\Gamma_1(\vec{q},\omega)=\frac{1}{N}\sum_{\vec{q}'}\int_{-\infty}^{\infty}\frac{d\omega'}{\pi}[V(\vec{q}')-V(\vec{q}'-\vec{q})]^2\times g_1(\vec{q}'\omega')g_1(\vec{q}-\vec{q}',\omega-\omega')\,, \tag{22}$$

$$\Gamma_2(\vec{q},\omega)=\frac{6}{N}\sum_{\vec{q}'}\int_{-\infty}^{\infty}\frac{d\omega'}{\pi}[V(\vec{q}')]^2\times g_1(\vec{q}',\omega')g_2(\vec{q}-\vec{q}',\omega-\omega')\,. \tag{23}$$

Thus Eqs. (19)–(23) give the nonlinear integral equations for G_1 and G_2.

In general, solving these sets of four-variable nonlinear integral equations could be very difficult. However, we note that the approximation which generates these equations gives expressions for the moments that are no more accurate than $1/c$, where c is the number of nearest neighbors.[21] Thus a solution to Eqs. (22) and (23) that is good to order $1/c$ is almost as good as an exact solution. It will be shown below that a reduced non-variable integral equation will give one such solution.

In order to obtain this derived result, first consider the recursion relationships

$$L_1(\vec{q},2n+2)=\frac{1}{N}\sum_{\vec{q}'}[V(\vec{q}')-V(\vec{q}'-\vec{q})]^2\times\sum_{l=0}\binom{2n}{2l}M_1(\vec{q}',2l)M_1(\vec{q}-\vec{q}',2n-2l), \tag{24a}$$

$$L_2(\vec{q},2n+2)=\frac{6}{N}\sum_{\vec{q}'}[V(\vec{q}')]^2\times\sum_{l=0}^{n}\binom{2n}{2l}M_1(\vec{q}',2l)M_2(\vec{q}-\vec{q}',2n-2l)\,, \tag{24b}$$

which are generated by taking the even moments of Eq. (22) and (23), since the odd moments of G_α and Σ_α are zero in the absence of an external field. Equations (24) together with Eq. (7), which is rewritten

$$M_\alpha(\vec{q},2n+2)=\sum_{m=1}^{n+1}L_\alpha(\vec{q},2m)M_\alpha(\vec{q},2n+2-2m)\,, \tag{25}$$

and the fact that $M_\alpha(\vec{q},0)=1$ is enough to generate all of the moments of G_α in the bubble approximation. We also note that

$$N^{-1}\sum_{\vec{q}}V(\vec{q}-\vec{q}_1)V(\vec{q}-\vec{q}_2)\cdots V(\vec{q}-\vec{q}_n)=\sum_{\vec{l}}[V(\vec{l})]^n\exp[i(\vec{q}_1+\vec{q}_2+\cdots+\vec{q}_n)\cdot\vec{l}]\alpha cV_0^n\,, \tag{26}$$

where V_0 is the nearest-neighbor interaction strength. It is also convenient to define

$$V_2(\vec{q})=N^{-1}\sum_{\vec{q}'}[V(\vec{q}')-V(\vec{q}'-\vec{q})]^2\,,=2\sum_{\vec{l}}[V(\vec{l})]^2(1-e^{i\vec{q}\cdot\vec{l}})\,. \tag{27}$$

The most important contributions to $L_1(\vec{q},2k)$ will come from factors like those in Eq. (26) with $n=2$ rather than from factors with $n<2$. This is simply because this will lead to the lowest power of $1/c$. Now, because of the factor $[V(\vec{q}')-V(\vec{q}'-\vec{q})]^2$ in Eq. (25), it is seen that only those parts of $M_1(\vec{q},2k)$ that are independent of $\vec{q}$ will contribute to L_1 to lowest order in $1/c$. Thus the set of $\vec{q}$-independent parts of the moments $M_1(\vec{q},n)$ can be used to generate an approximation to Γ_1 through Eq. (24a) which is correct to order $1/c$ at all wavelengths. It is further convenient to use dimensionless variables so that frequencies are measured relative to V where

$$V^2=\frac{2}{N}\sum_{\vec{q}}V^2(\vec{q})\,. \tag{28}$$

The dimensionless equations which generate the $\vec{q}$-dependent moments are

$$\tilde{\Gamma}_1(y)=\int\frac{dy'}{\pi}\tilde{g}_1(y')\tilde{g}_1(y-y')\,,$$
$$\tilde{g}_1(y)=\tilde{\Gamma}_1(y)/\{[y-\tilde{\Pi}_1(y)]^2+\tilde{\Gamma}_1^2(y)\}\,, \tag{29}$$
$$\tilde{\Pi}_1(y)=-P\int\frac{dy'}{\pi}\tilde{\Gamma}_1(y')/(y-y')\,,$$

where P denotes the principal part of the integration, y is the dimensionless frequency ω/V, and the tilde denotes that the quantities are in the dimensionless form described above. In this approximation, $\Gamma_1(\vec{q}\omega)$ is then given by

$$\Gamma_1(\vec{q},\omega)=V_2(\vec{q})\tilde{\Gamma}_1(y)/V\,. \tag{30}$$

This solution reproduces correctly all the moments of $\Gamma_1(\vec{q},\omega)$ to order $1/c$ for all values of $\vec{q}$ and thus the spin-diffusion coefficient should also be correct to this order.

A similar argument can be made for the quadrupolar correlation function G_2 with the $\vec{q}$-independent moments being generated by the equations

$$\tilde{\Gamma}_2(y)=3\int\frac{dy'}{\pi}\tilde{g}_1(y')\tilde{g}_2(y-y')\,,$$
$$\tilde{g}_2(y)=\tilde{\Gamma}_2(y)/\{[y-\tilde{\Pi}_2(y)]^2+\tilde{\Gamma}_2^2(y)\}\,, \tag{31}$$

$$\tilde{\Pi}_2(y) = -P\int \frac{dy'}{\pi}\,\tilde{\Gamma}_2(y')/(y-y').$$

In this case, however, the actual correlation function is independent of $\vec{q}$ to order $1/c$ and

$$\Gamma_2(\vec{q},\omega) = V\tilde{\Gamma}_2(y)\ . \tag{32}$$

Equations (29) and (31) have been solved on a computer numerically by iteration. The real and imaginary parts of the self-energies are plotted in Figs. 4 and 5. For values of $y < 4$, the Gaussian functions

$$\tilde{\Gamma}_1(y) = (\pi^{1/2}/2)\,e^{-y^2/4}\ ,$$
$$\tilde{\Gamma}_2(y) = (3\pi^{1/2}/2^{3/2})\,e^{-y^2/8}\ , \tag{33a}$$

give reasonably good fits to the curves. On the other hand, for $y < 8$, the spectral functions decrease exponentially as

$$\tilde{g}_1(y) = 6\pi\,|y|\,e^{-2.79|y|}\ ,$$
$$\tilde{g}_2(y) = 8.99\,|y|\,e^{-2.43|y|}\ . \tag{33b}$$

The solution for $\tilde{\Gamma}_2(y)$ and $\tilde{g}_2(y)$ are the first such results obtained for the quadrupole correlation function.

Equation (22) has been solved in the time domain by Blume and Hubbard[11] by an iteration technique. Our solution is in the frequency domain, and further, is good only to order $1/c$ for the dipole correlation function. To our knowledge, it is the first self-consistent solution in the frequency domain. The solution given by Eq. (30) describes a correlation function which is the same as that of Blume and Hubbard at all wavelengths to within corrections of order $1/c$.

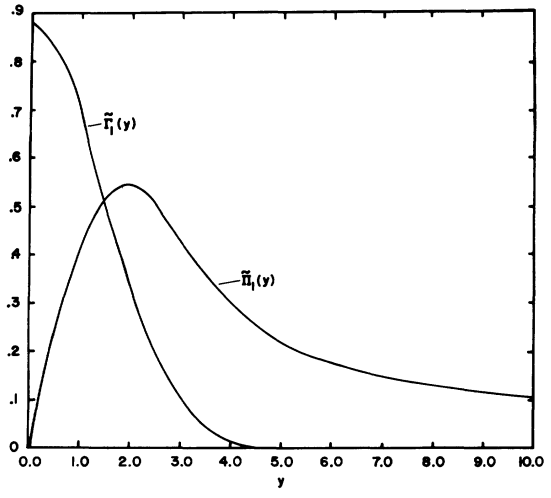

FIG. 4. The real and imaginary parts, $\tilde{\Pi}_1(y)$ and $\tilde{\Gamma}_1(y)$, of the $\vec{q}$-independent dipole correlation function self-energy.

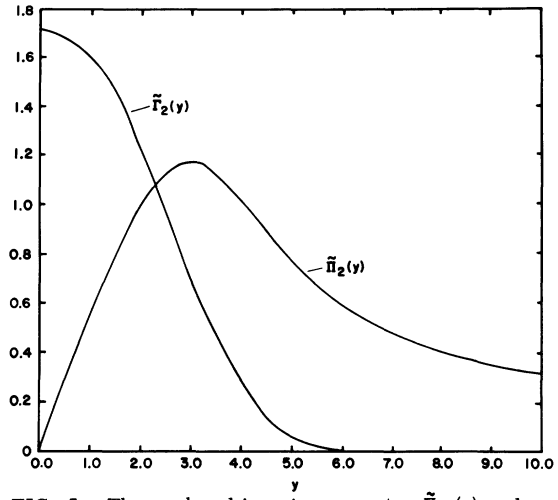

FIG. 5. The real and imaginary parts, $\tilde{\Pi}_2(y)$ and $\tilde{\Gamma}_2(y)$, of the $\vec{q}$-independent quadrupole correlation function self-energy.

B. Diffusion coefficient and exchange-narrowed dipolar linewidth; experimental comparison

Since, by Eq. (32), $\Gamma_2(\vec{q},\omega)$ is independent of wave vector to order $1/c$, the solutions $\tilde{\Gamma}_2(y)$, $\tilde{\Pi}_2(y)$, and $\tilde{g}_2(y)$ are the best solutions that one can obtain to that order of accuracy. Any $\vec{q}$ dependence would enter into these quadrupolar functions in higher orders of $1/c$. On the other hand, the dipole function $\Gamma_1(\vec{q},\omega)$ given by Eq. (30), retains a wave-vector dependence even to order $1/c$. In order to obtain an improved solution which is a better approximation to $\Gamma_1(\vec{q},\omega)$ than that given by Eq. (30), one first approximates Eq. (22) in the following form:

$$\Gamma_1(\vec{q},\omega) = \frac{1}{2}\sum_{\vec{q}'}[V(\vec{q}') - V(\vec{q}'-\vec{q})]^2\gamma(\vec{q}',\omega)\,, \tag{34}$$

where $\gamma(\vec{q},\omega)$ is defined as

$$\gamma(\vec{q},\omega) = \int_{-\infty}^{\infty}\frac{d\omega'}{\pi}\,g_1(\vec{q},\omega')g_1(\vec{q},\omega-\omega')\,. \tag{35}$$

In other words, the $\vec{q}$ dependence of the second spectral function in Eq. (22) has been neglected, but the $\vec{q}'$ dependence has been retained. This procedure can be justified, in the low-$\vec{q}$ limit desirable for the diffusion coefficient calculation, if it is noted that in Eq. (22) the sum is over all wave vectors $\vec{q}'$ in the first Brillouin zone. The major contribution to such a sum will come from the region where $|\vec{q}'| \gg |\vec{q}|$ if $|\vec{q}|$ is small compared to the Debye cutoff q_D. This condition will always be valid for experimental EPR conditions and in the low-$\vec{q}$ region where spin diffusion is important.

The second step necessary to obtain a better $\vec{q}$-dependent solution is to substitute Eq. (30) into Eq. (21) to obtain a $\vec{q}$-dependent spectral function

$g_1(\vec{q},\omega)$. The resulting spectral function is then substituted into Eq. (35) to obtain the function $\gamma(\vec{q},\omega)$. This procedure has been carried out numerically by using the computer result discussed above for $\tilde{\Gamma}_1(y)$ and by treating the quantity

$$\alpha(\vec{q}) \equiv V_2(\vec{q})/V^2 , \tag{36}$$

which occurs in Eq. (30), as a parameter. $\gamma(\vec{q},\omega)$ has been evaluated numerically for various values of the parameter α and for various frequencies. The results of this calculation are discussed in detail in Ref. 21. The explicit $\vec{q}$ dependence of $\gamma(\vec{q},\omega)$ can be found for a given ω by first fitting the numerical results for $\gamma(\vec{q},\omega)$ to a polynomial in $\alpha(\vec{q})$ and then by substituting the functional form of $\alpha(\vec{q})$ into the polynomial. This functional form is known through Eqs. (27) and (36) once the form of the interaction, $V(\vec{q})$, has been specified. Finally, this polynomial form of the function $\gamma(\vec{q},\omega)$ is substituted into Eq. (34), and the $\vec{q}'$ sum is explicitly performed for each specific ω and for a specific form of the interaction. Since, for the calculation of the spin-diffusion coefficient, we are only interested in the $\omega = 0$ limit of Eqs. (34) and (35) and in the small-$\vec{q}$ limit of Eq. (34), only these cases will be considered here. When fit to a polynomial in $\alpha(\vec{q})$, the function $\gamma(\vec{q},\omega)$ takes the form[21]

$$\gamma(\vec{q},\omega=0) = \{0.4852 + 0.0558\alpha(\vec{q}) + 0.0039\,[\alpha(\vec{q})]^2 + 0.5642/\alpha(\vec{q})\}/V. \tag{37}$$

This form fits the computer-generated function to within 0.1% for all values of $\alpha(\vec{q})$.

In order to calculate the diffusion coefficient from Eq. (37) and the $\omega = 0$ limit of Eq. (34), we have considered a simple cubic lattice with only near-neighbor exchange. This is a good approximation for dense magnetic insulators of the perovskite structure such as $RbMnF_3$.[6] (The Mn^{++} ions form a simple cubic lattice with each other.) In this case, the interaction takes the form[9]

$$V(\vec{q}) = 4[S(S+1)/3]^{1/2} J \sum_i \sin^2(\tfrac{1}{2}q_i a) \tag{38}$$

where J is the nearest-neighbor exchange constant, a is the lattice spacing, q_i is the ith component of $\vec{q}$, and the sum goes over the Cartesian indices (x,y,z). When this interaction is substituted into Eqs. (37) and (36), the $\omega = 0$ limit of Eq. (34), and the q' sum is performed, the result in the low-q limit ($|\vec{q}|a \ll 1$) has the form

$$\Gamma_1(\vec{q},0) = D(\vec{q})^2 , \tag{39}$$

where D is, by definition, the diffusion coefficient[9,18] and explicitly takes the form

$$D = 0.376[S(S+1)]^{1/2} Ja^2 . \tag{40}$$

This result is in the range of previous theoretical estimates for D.[9,11,22]

We have evaluated D for $RbMnF_3$ using the parameters $S = \frac{5}{2}$, $a = 4.239$ Å,[23] and $J = 0.568$ MeV.[24] The result is

$$D = 11.37 \text{ MeV Å}^2 = 1.726\times10^{-3} \text{ cm}^2/\text{sec}. \tag{41}$$

This result is 11.5% lower than the latest experimental value, obtained by Tucciarone, Hastings, and Corliss,[15] of 12.86 ± 0.21 MeV Å.[2] This is good agreement in our case, since the equations from which D was derived are accurate only to order $1/c$, which for a simple cubic lattice means that the expected accuracy of the prediction should be only around 16%. Therefore, our results for D, which, it should be reemphasized, were obtained in lowest-order *self-consistent* approximation, give a prediction in reasonable agreement with experiment and in good agreement with previous theoretical estimates.

The exchange-narrowed dipolar linewidth of the Heisenberg paramagnet has long been of theoretical interest[3,25-27] and has only recently been approached from a microscopic viewpoint.[6] This linewidth is experimentally observable in dense magnetic insulators, and has been measured via EPR in $RbMnF_3$.[7] It is possible to calculate such a dipolar linewidth by use of the above self-consistent results for the function $\gamma(\vec{q},\omega)$, defined in Eq. (35), which were obtained for isotropic exchange.

The dipolar interaction, as has been discussed earlier, contributes a term of the form shown in Eq. (14) to the Hamiltonian of the system. Consider, now, the corresponding-spin self-energy function as given in Eq. (16). When the imaginary part of the equation is taken, one obtains a similar equation which gives the linewidth function $\Gamma_{11}(\vec{q},\omega)$ in terms of the various spectral functions $g_{\alpha\beta}(\vec{q},\omega)$. Of course each $g_{\alpha\beta}(\vec{q},\omega)$ is related to its corresponding $\Gamma_{\alpha\beta}(\vec{q},\omega)$ by an equation similar to Eq. (21). Now, in general, $J(\vec{q}) \gg I_{ij}(\vec{q})$ so, except near $\vec{q} \equiv 0$, the major contribution to $\Gamma_{\alpha\beta}(\vec{q},\omega)$ is given by Eq. (22) and an excellent approximation to $g_{\alpha\beta}(\vec{q},\omega)$ is its diagonal part, given by Eq. (21). In other words, it is reasonable, for $\vec{q} \neq 0$, to neglect the dependence of $\Gamma_{\alpha\beta}(\vec{q},\omega)$ and thus $g_{\alpha\beta}(\vec{q},\omega)$ on $I_{ij}(\vec{q})$ when the spectral functions that enter the imaginary part of Eq. (16) are being calculated. A reasonable

TABLE I. Exchange-narrowed dipolar linewidth.

Number of neighbor shells included	$\dfrac{J\Gamma_D a^6}{[S(S+1)]^{1/2}\hbar^4\gamma_e^4}$	Γ_D for $RbMnF_3$ (G)
1	9.1712	32.75
2	11.3594	40.56
3	12.2916	43.89
4	12.8675	45.94
5	12.8195	45.77

approximation to make in Eq. (16) is therefore to let all $G_{\alpha\beta}(\vec{q},\omega)$ that occur there be replaced by the isotropic function $G_1(\vec{q},\omega)$, since whenever such functions occur all wave vectors are being summed over.

Since the dipolar linewidth is only appreciable in the $|\vec{q}|=0$, $\omega=0$ region, that is the only region we will consider here. So, when the imaginary part of Eq. (16) is taken, when all spectral functions are approximated by the isotropic spectral function, and when the $|\vec{q}|=0$, $\omega=0$ limits are taken, the result for the dipolar linewidth is

$$\Gamma_D \equiv \Gamma_1(\vec{q}=0,\omega=0) = \left(\frac{S(S+1)}{3}\right)^{1/2} \frac{1}{N}\sum_{\vec{q}} \{[I_{xx}(\vec{q}) - I_{yy}(\vec{q})]^2 + 4[I_{xy}(\vec{q})]^2 + [I_{xz}(\vec{q})]^2 + [I_{yz}(\vec{q})]^2\}\gamma(\vec{q},0) \ , \tag{42}$$

where $\gamma(\vec{q},0)$ is given explicitly by Eq. (37). A similar equation has been obtained by Huber[28] for temperatures near the critical point, but in our case we know $\gamma(\vec{q},0)$ self-consistently and we are only considering the high-temperature limit. The task of calculating Γ_D has now been reduced to evaluating the wave-vector sum which occurs in Eq. (42).

Since forces beyond near-neighbor forces are appreciable for the dipolar interaction, we have performed this wave-vector sum for a simple cubic lattice including first- through fifth-neighbor forces. The results with the inclusion of each succeeding shell of neighbors are shown in column two of Table I. The differences between succeeding approximations to Γ_D appear to be getting smaller the larger the number of shells included. If the fourth- to fifth-neighbor difference is any indication, these numbers will also begin to oscillate as more shells are included. However, it is not obvious to what number the result is converging. Unfortunately, the more shells that are included, the more cumbersome the calculations become and the more complicated $I_{ij}(\vec{q})$ becomes.

The experimentally measured linewidth Γ_D for $RbMnF_3$ is 58 G (1.0×10^9 sec^{-1}).[7] We have calculated Γ_D for $RbMnF_3$ using the theoretical results shown in column two of Table I. The results for the inclusion of each succeeding neighbor shell are shown in column three of the same table. As was mentioned above, these numbers appear to be getting closer together as more shells are included; however, it is not obvious (or even likely) that they are converging to the experimental number. Certainly, one would again naively expect a theoretical number in error by at least the order of $1/c$, since the original equations which were used to obtain Γ_D are only accurate to that order. The inclusion of the fifth shell, as is shown in Table I, gives a dipolar linewidth of $\Gamma_D = 45.77$ G, which is within 22.1% of the experimental value. Better agreement with experiment could possibly be achieved if the equations could be improved to include higher order in $1/c$.

Our calculation of Γ_D is self-consistent in the sense that the isotropic exchange has been taken into account self-consistently. As far as we can determine, ours is the first such self-consistent calculation of Γ_D. By not taking into account the dipolar interaction self-consistently, we have made an error of the order of $\Gamma_D/D|\vec{q}|^2$ in calculating the spectral function $g_1(\vec{q},\omega)$, which we used in Eqs. (35) and (42). Here D is the spin-diffusion coefficient calculated above. The dipolar interaction will therefore only matter when the ratio is not much less than 1. Using the theoretical expressions for D and Γ_D that were obtained above along with the experimental values for J and a in $RbMnF_3$, it can be seen that such a situation will occur only for $|\vec{q}|a > 10^{-2}$. This condition will hold only in a volume in q space of around 10^{-6} of the volume of the first Brillouin zone. Since all wave vectors are summed over in Eq. (41), Γ_D is indeed negligible in the calculation of the spectral function that one uses in that equation.

Finally, a comment should be made regarding the calculations of the two-point quadrupolar correlation function which were presented in this section. These calculations, which to our knowledge constitute the first accurate treatment of this function, indicate that the usual approximation, which treats the function as a decomposition of dipolar correlation functions,[5,15] is not a valid approximation for the Heisenberg paramagnet. In addition, the method of generating integral equations from infinite sets of moments should be applicable to a large number of problems involving spins in the high-temperature limit. These are just those problems for which it is very difficult to generate self-energy perturbation theories by the usual methods.

---

*Based in part upon a portion of the Doctoral dissertation presented by C. W. Myles to the Department of Physics, Washington University.

†Research supported in part by the National Science Foundation

‡Major portion of the work completed while a National Science Foundation Predoctoral Trainee.

§Present address.

[1]P. de Gennes, J. Chem. Phys. Solids 4, 223 (1958).

[2]H. Mori and K. Kawasaki, Prog. Theor. Phys. (Kyoto) 27, 529 (1962).

[3]See, for example, J. E. Gulley, D. Hone, D. J. Scala-

pino, and B. G. Silbernagel, Phys. Rev. B 1, 1020 (1970).
[4]P. Resibois and M. De Leneer, Phys. Rev. 178, 806 (1969).
[5]G. F. Reiter, Phys. Rev. B 5, 222 (1972).
[6]P. A. Fedders, Phys. Rev. B 3, 2352 (1971).
[7]J. E. Gulley, B. Silbernagel, and V. Jaccarino, J. Appl. Phys. 40, 1318 (1969).
[8]J. G. Miller, P. A. Fedders, and D. I. Bolef, Phys. Rev. Lett. 27, 1063 (1971).
[9]H. S. Bennett and P. C. Martin, Phys. Rev. 138, A 608 (1965).
[10]The first calculations of a frequency dependent spectral density were done by F. Wegner, Z. Phys. 216, 443 (1968); Z. Phys. 218, 260 (1969).
[11]M. Blume and J. Hubbard, Phys. Rev. B 1, 3815 (1970).
[12]G. F. Reiter, Phys. Rev. B 7, 3325 (1973).
[13]D. L. Huber, Phys. Rev. B 6, 3180 (1972).
[14]C. G. Windsor, Proc. R. Soc. Lond. 91, 353 (1967).
[15]A. Tucciarone, J. M. Hastings, and L. M. Corliss, Phys. Rev. Lett. 26, 252 (1971); Phys. Rev. B 8, 1103 (1973).
[16]P. A. Fedders, Phys. Rev. B 5, 181 (1972).
[17]See, for example A. A. Abrikosov, L. P. Gorkov, and I. E. Dzyaloshinski, *Quantum Theoretical Methods in Statistical Physics* (Pergamon, New York, 1965).
[18]L. P. Kadanoff and P. C. Martin, Ann. Phys. (N.Y.) 24, 419 (1963).
[19]H. S. Bennett and E. Pytte, Phys. Rev. 155, 553 (1967).
[20]By irreducible diagrams we mean diagrams that are still connected if a single line is cut. See, for instance, Ref. 5.
[21]C. W. Myles, Ph.D. dissertation (Washington University, St. Louis, Mo. 1973) (unpublished).
[22]T. Morita, Phys. Rev. B 6, 3385 (1972).
[23]R. L. Melcher, Ph.D. dissertation (Washington University, St. Louis, Mo. 1968) (unpublished).
[24]C. G. Windsor, G. A. Briggs, and M. Kestigan, J. Phys. C 1, 940 (1968).
[25]J. H. Van Vleck, Phys. Rev. 74, 1169 (1948).
[26]P. W. Anderson and P. R. Weiss, Rev. Mod. Phys. 25, 269 (1953).
[27]R. Kubo and K. Tomita, J. Phys. Soc. Jap. 9, 888 (1954).
[28]D. L. Huber, J. Phys. Chem. Solids 32, 2145 (1971).